Agricultural Water Management 236 (2020) 106164

Contents lists available at ScienceDirect

Agricultural Water Management

journal homepage: www.elsevier.com/locate/agwat

Evapotranspiration partitioning and crop coefficient of maize in dry semi-humid climate regime

Yunfei Wang[a,b,c], Huanjie Cai[a,b,*], Lianyu Yu[c], Xiongbiao Peng[a,b], Jiatun Xu[a,b], Xiaowen Wang[a,b]

[a] Key Laboratory of Agricultural Soil and Water Engineering in Arid Area of Ministry of Education, Northwest Agriculture and Forestry University, Yangling, China
[b] Institute of Water Saving Agriculture in Arid Regions of China (IWSA), Northwest Agriculture and Forestry University, Yangling, China
[c] Faculty of Geo-Information Science and Earth Observation, University of Twente, Enschede, the Netherlands

ARTICLE INFO

Keywords:
Evapotranspiration partitioning
Energy fluxes
Crop coefficient
Eddy covariance

ABSTRACT

Guanzhong Plain is one of the most critical maize production areas in Northwest China. It is essential to study the maize irrigation requirement and improve water use efficiency in this area. There is a lack of knowledge about the evaporation portioning and irrigation requirements of crops grown in this region. Based on evapotranspiration observed in a maize cropland using the eddy covariance (EC) technique during four growing seasons (2013, 2014, 2015, and 2017), the seasonal variation of evapotranspiration components and the crop coefficients (K_c) for summer maize in a dry semi-arid area were determined. Energy partitioning has an obvious seasonal variation during growing seasons. The pattern of evapotranspiration partitioning has a clear seasonal variation with the development of the canopy. The pattern of the ratio of transpiration (T) to evapotranspiration (ET) is consistent with the canopy development. For four growing seasons, on a seasonal basis, the ratios of T to ET and E to ET were comparable. In addition, the locally developed crop coefficients were 0.57, 1.01, and 0.50 for the initial, mid, and late stages, respectively. The single crop coefficient derived from local datasets can provide a good prediction of ET. The K_c values reported in this paper were consistent with previous studies conducted in other regions using EC systems but were generally lower than the K_c values derived from ET data measured by lysimeters, the Bowen Ratio Energy Balance system, and the soil water balance method. This indicates that the variability of the locally developed crop coefficient caused by measurement methods is higher than the variability caused by climate.

1. Introduction

Evapotranspiration plays an important role in the balance of water and energy in agricultural ecosystems (Wang et al., 2019; Zhu et al., 2016). In areas where water resources are scarce, an in-depth study of evapotranspiration is essential for optimal water use and management. To predict crop water requirements, it is essential to calculate the crop evapotranspiration (ET_c) (Allen et al., 2011; Sun et al., 2012). The most widely used practical method for predicting ET_c is the single crop coefficient method, which was reported by Allen et al. (1998) in the FAO-56 document. This method is mainly used for irrigation management, and it has been applied in different agroecosystems all over the world. However, many studies have evidenced that the FAO-provided crop coefficient values for different regions are unreasonable, so it is necessary to develop crop coefficients based on local datasets (Facchi et al., 2013; Gong et al., 2017; Kang et al., 2003; Li et al., 2008, 2003; Parkes et al., 2005; Piccinni et al., 2009; Sánchez et al., 2014; Wang et al., 2019; Xu et al., 2018; Yang et al., 2016).

Although the weighing lysimeter is widely used to measure ET and calculate K_c, its representative area is too small (Rana and Katerji, 2000; Alfieri et al., 2012). Another common method is eddy covariance (EC), which can be used to accurately measure ET in a short time interval (e.g. 30 min), and its representative area is much larger than that of a lysimeter (Baldocchi, 2003). However, there are few studies on the determination of summer maize crop coefficient and ET partitioning using the EC method in Guanzhong Plain, northwest China.

The Guanzhong Plain is an important food-production area of China which accounts for about two-thirds of the total crop yield in Shannxi province (Zhao et al., 2018), and summer maize (*Zea mays* L.) is one of the most planted crops in this region (Li et al., 2016). Although some previous studies have reported the crop coefficient of summer maize in this area, they were all based on ET data measured by lysimeter or water balance methods (Kang et al., 2003; Parkes et al., 2005). Since June 2013, long-term observations of ET as well as meteorological and

* Corresponding author at: Institute of Water Saving Agriculture in Arid Regions of China, Northwest A&F University, 712100, Yangling, China.
E-mail address: caihj@nwsuaf.edu.cn (H. Cai).

https://doi.org/10.1016/j.agwat.2020.106164
Received 26 March 2019; Received in revised form 24 February 2020; Accepted 22 March 2020
Available online 07 April 2020
0378-3774/

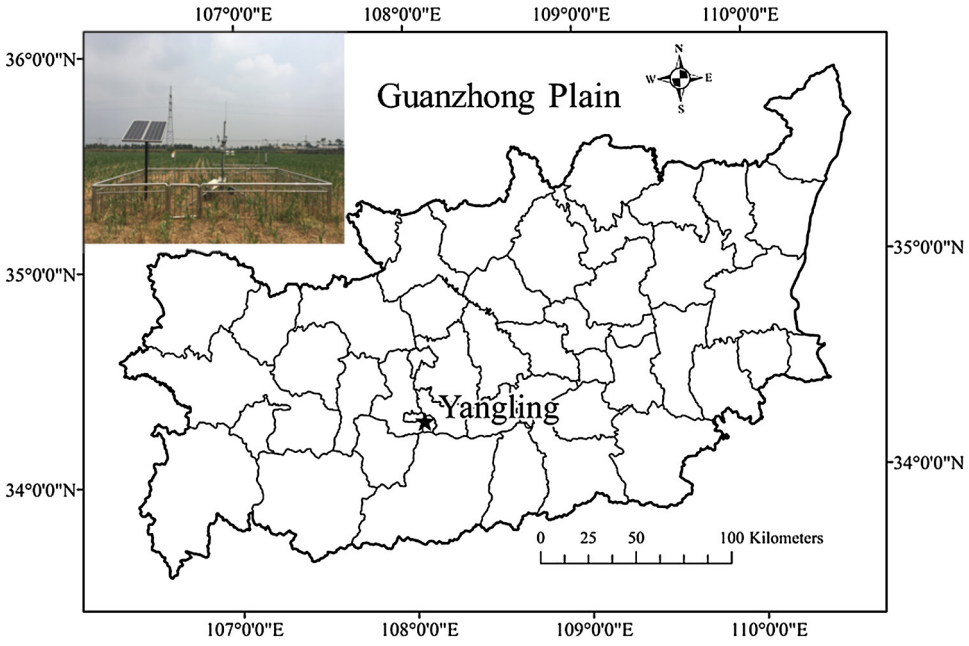

Fig. 1. Location of the research site near Yangling, Shaanxi Province, China. The photo inset shows the eddy covariance flux tower.

biological factors have been carried out in a summer maize field in Guanzhong Plain.

In this study, water and energy fluxes were observed based on eddy covariance techniques in a maize cropland ecosystem in the dry semi-humid region of northwestern China. The objectives of our study were (1) to examine the reliability of the eddy covariance technique to measure *ET*; (2) to study the diurnal and seasonal variations of energy fluxes and the seasonal variations of evapotranspiration partitioning in maize fields; and (3) to determine the local K_c curve and study its controlling factors and then predict crop water requirements for maize in Guanzhong Plain.

2. Materials and methods

2.1. Location and site information

This experiment was conducted at the experiment field of Northwest A&F University (34°17′ N, 108°04′ E, 521 m a.s.l.) during June 2013 to June 2018 (Fig. 1). The experiment field was approximately 200 m (north to south) by 250 m (east to west). The soil in the study area was silty clay loam, the field capacity was 0.42 m^3 m^{-3}, the permanent wilting point was 0.0875 m^3 m^{-3}, and the bulk density was 1.35 g cm^{-3}. The depth of groundwater through capillary action level was more than 55 m. Thus, the water supplied by groundwater was assumed to be equal to zero. The mean annual temperature was 12.9 °C, and the mean annual precipitation was 630 mm (Yu et al., 2016, 2018). The mean annual precipitation was 599 mm during the period of observation. The wetter years were 2016 and 2017, the drier years were 2013 and 2015, and 2014 was a relatively normal precipitation year (Table 1). The cultivar of maize was Wuke No. 2, and the maximum crop height was about 190 cm in the summer maize season. The schedule of management activities is shown in Table 2. The field management schedule (i.e., application of fertilizer, weed control, and irrigation) was based on the local standard management schedule (Table 2). Nitrogen (N) was applied as a urea ammonium nitrate solution, and typically 180 kg N/ha was applied before sowing the summer maize. Flood irrigation was implemented when the crops were under slight water stress (i.e., when the soil moisture was less than 50 % of plant available water), and the amount of irrigation was determined by the evapotranspiration and precipitation measured by EC tower after the last irrigation (Yu et al., 2016, 2018).

2.2. Field measurements

The EC system was installed on a height-adjustable tripod. The sensors were positioned 3 m above the soil surface during the maize growing season. The EC system included a three-dimensional sonic anemometer (CSAT-3, Campbell Scientific, Logan, UT, USA) pointed toward the prevailing wind direction, an open path infrared gas analyzer (LI-7500A, LI-COR, Lincoln, NE, USA), and a data logger (LI7550, 10 Hz, LI-COR, Lincoln, NE, USA). The objective of this system was to measure both water and carbon fluxes between ecosystem and atmosphere. Net radiation was measured by a four-Component net radiometer installed 2.5 m above the soil surface. The boundary layer meteorological measurements, including wind speed and wind direction, were measured with propeller anemometers (R.M. Young model 03002-5, available from Campbell Scientific), and the air temperature and relative humidity were measured with a humidity and temperature probe (model HMP60, Vaisala, Finland). All signals were logged by a CR1000 data logger (Campbell Scientific) and recorded at 30 min intervals. Soil temperature and soil volumetric water content observations were taken at three depths (20, 40, and 60 cm below the soil surface) using a model 5TM dielectric permittivity meter (METER Environment, Pullman, WA, USA). Rainfall was measured by a tipping bucket rain gauge (model TE525MM-L, available from Campbell Scientific), snowfall was measured by a weighing type precipitation gauge (model OTT Pluvio, Dusseldorf, Germany), and soil heat flux (G) was measured with a self-tuning heat flux plate (model HFP01SC-L50, Hukseflux, Delft, The Netherlands) at 8 cm below the soil surface. All sensors were calibrated and validated before installation.

2.3. Flux data processing

EddyPro software (https://www.licor.com/env/products/eddy_covariance/software.html) was used to process observed data into 30-min interval turbulent latent (*LE*) and sensible heat fluxes (*H*). Post-processing of EC data included (1) spike detection, (2) time lag correction of H_2O/CO_2, (3) frequency response correction, and (4) coordinate rotation using the planar fit method presented by Wilczak et al. (2001). Additionally, during the calculation of flux data, density

Table 1
Meteorological conditions, reference evapotranspiration (ET_0), measured evapotranspiration (*ETa*), evaporation (*E*), and transpiration (*T*) in maize season during four years (2013, 2014, 2015, and 2017).

Year	Stage	Days d	*Tair* ^{0}C	*Ws* m^{-s}	*VPD* kPa	*Rn* W m^{-2}	*SWC_20* m^3 m^{-3}	*SWC_40* m^3 m^{-3}	*P* mm	ET_0 mm day^{-1}	*ETa* mm day^{-1}	*E* mm day^{-1}	*T* mm day^{-1}	*T/ETa*
2013	Ini	20	27.2	1.26	1.37	117.3	25.8	29.1	25.4	3.68	2.51	1.94	0.56	0.22
	Dev	30	25.9	0.68	0.79	122.7	26.7	29.4	109.6	3.38	2.99	0.91	2.07	0.69
	Mid	51	23.3	0.28	0.90	82.6	25.6	28.4	74.5	2.24	2.10	1.00	1.14	0.54
	Lat	10	19.5	0.68	0.86	68.7	26.1	30.3	0.0	2.12	1.56	1.39	0.17	0.11
	Seasonal	111	24.4	0.60	0.95	98.4	26.0	29.0	209.5	2.80	2.36	1.18	1.20	0.50
2014	Ini	28	27.5	1.00	1.64	130.8	24.5	26.8	39.0	4.06	2.19	1.81	0.38	0.17
	Dev	21	26.2	0.77	1.32	112.3	21.9	26.9	62.3	3.42	2.22	1.16	1.06	0.48
	Mid	50	20.7	0.44	0.49	88.3	21.8	29.9	275.1	2.31	2.24	0.60	1.64	0.73
	Lat	7	17.7	0.40	0.47	79.5	21.3	30.6	0.0	2.03	1.87	0.74	1.14	0.61
	Seasonal	106	23.4	0.66	0.96	103.7	22.5	28.5	376.4	2.97	2.20	1.04	1.16	0.52
2015	Ini	20	23.8	0.74	0.82	109.8	23.1	25.9	82.0	3.05	2.20	1.94	0.48	0.22
	Dev	30	26.9	0.93	1.38	151.6	22.7	26.4	45.8	4.43	3.26	1.63	1.63	0.50
	Mid	45	22.2	0.50	0.73	111.5	21.8	24.2	131.0	3.06	3.01	1.10	1.98	0.66
	Lat	16	16.0	0.48	0.35	46.7	25.5	25.0	19.4	1.31	1.19	0.78	0.47	0.39
	Seasonal	111	22.9	0.66	0.87	112.6	22.8	25.2	278.2	3.18	2.67	1.34	1.42	0.51
2017	Ini	20	26.8	0.93	1.77	154.2	16.4	18.5	21.0	4.76	3.10	2.64	0.46	0.15
	Dev	30	29.2	1.08	1.86	166.2	19.6	21.1	62.5	5.30	3.45	1.84	1.44	0.42
	Mid	45	22.2	0.31	0.61	98.0	20.2	21.3	95.2	2.65	2.62	0.48	2.13	0.81
	Lat	16	16.2	0.35	0.15	44.4	23.7	22.1	125.7	1.17	0.82	0.33	0.48	0.58
	Seasonal	111	24.0	0.63	1.09	118.8	19.9	20.9	304.4	3.53	2.69	1.22	1.41	0.54

Ini, Dev, Mid, and Lat mean the initial, development, mid, and late growth stages, respectively. *Tair* is the air temperature, *Ws* is the wind speed at 2 m, *VPD* is the vapor pressure deficit, *Rn* is the net radiation, *SWC_20* and *SWC_40* are the volumetric soil water content at 20 cm depth and 40 cm depth, respectively, *P* is the precipitation, ET_0 is the reference evapotranspiration, *ETa* is the measured evapotranspiration, *E* is the soil evaporation, *T* is the transpiration, *T/ETa* is the ratio of transpiration to evapotranspiration.

Table 2
The schedule of management activities in 2013, 2014, 2015, and 2017.

Year	Irrigation date	Volume (mm)	Sowing date	Harvest date
2013	16th August	93	21st June	9th October
2014	Rain-fed	0	26th June	9th October
2015	10th July	30	21st June	9th October
2017	21st July	64	21st June	9th October

correction was based on the method presented by Webb et al. (1980). The processed 30-min flux data and meteorological data were screened for anomalous or spurious values caused by system malfunction, power failure, and bad atmospheric conditions, and those data were excluded (Zhang et al., 2016). Based on the quality analysis by EddyPro software, approximately 23.1 % of the flux data recorded from 2013 to 2018 were deleted. Data gaps shorter than two hours were filled using linear interpolation, and data gaps longer than two hours were filled using the average daily variation method (Falge et al., 2001). As the low-quality data usually occurred in the evening, the systematic bias of filled data had limited effects on the water and energy flux analysis. Furthermore, regression analysis between the daily available energy (*Rn-G*) and the sum of sensible heat and latent heat (*H* + *LE*) was carried out since this method has been widely used to evaluate the energy-balance closure and the quality of EC data in previous studies. To overcome the energy imbalance issue, the Bowen ratio method was applied to correct the measured *ET* (Twine et al., 2000).

2.4. Adjustment of K_c values according to local conditions

To improve accuracy when using the single K_c method in a specific region, FAO-56 suggests using the observed durations of crop growth stages rather than the reference values. FAO-56 also provides equations to adjust the standard $K_{c\text{-}ini}$, $K_{c\text{-}mid}$, and $K_{c\text{-}lat}$ values according to local meteorological conditions, soil, irrigation, and management practices. The adjustment of $K_{c\text{-}ini}$ is based on the time interval between wetting events, the evaporation demand of the atmosphere, and the soil texture.

The equation for the adjustment of $K_{c\text{-}mid}$ is as follows:

$$K_{c-mid} = K_{c-mid(Tab)} + [0.04(u_2 - 2) - 0.004(RH_{min} - 45)]\left(\frac{h}{3}\right)^{0.3} \quad (1)$$

where $RH_{\min}$ is the mean value of the daily minimum relative humidity during the mid-season growth stage (%), u_2 is the mean value for the daily wind speed at a height of 2 m over the grass during the mid-season growth stage (m s^{-1}), and h is the mean crop height during the mid-stage (m) (Allen et al., 1998).

The adjustment for $K_{c\text{-}lat}$ is the same as for $K_{c\text{-}mid}$.

2.5. Calculations of parameters

The calculation of the crop coefficient (K_c) was as follows:

$$Kc = \frac{ET_c}{ET_0}, \quad (2)$$

where ET_c is the crop evapotranspiration measured by the EC system.

The equation used to calculate the reference evapotranspiration (ET_0) was as follows (ASCE-EWRI, 2005):

$$ET_0 = \frac{0.408\Delta(R_n - G) + \gamma(C_n/T + 273)u_2(e_s - e_a)}{\Delta + \gamma(1 + C_d u_2)}, \quad (3)$$

where R_n is the measured net irradiance at the crop canopy (MJ m^{-2} day^{-1}); G is the soil heat flux density (MJ m^{-2} day^{-1}); γ is the psychrometric constant (kPa °C^{-1}); C_n is the numerator constant (K mm s^3 mg^{-1} d^{-1}); u_2 is the mean daily wind speed at a height of 2 m (m s^{-1}); T is the measured mean daily air temperature (°C); e_s is the saturated vapor pressure (kPa); e_a is the mean actual vapor pressure (kPa); Δ is the slope of the saturation vapor pressure temperature curve (kPa °C^{-1}); and C_d is the denominator constant (s m^{-1}).

To reveal the annual and interannual variability in *ET*, we calculated the canopy conductance:

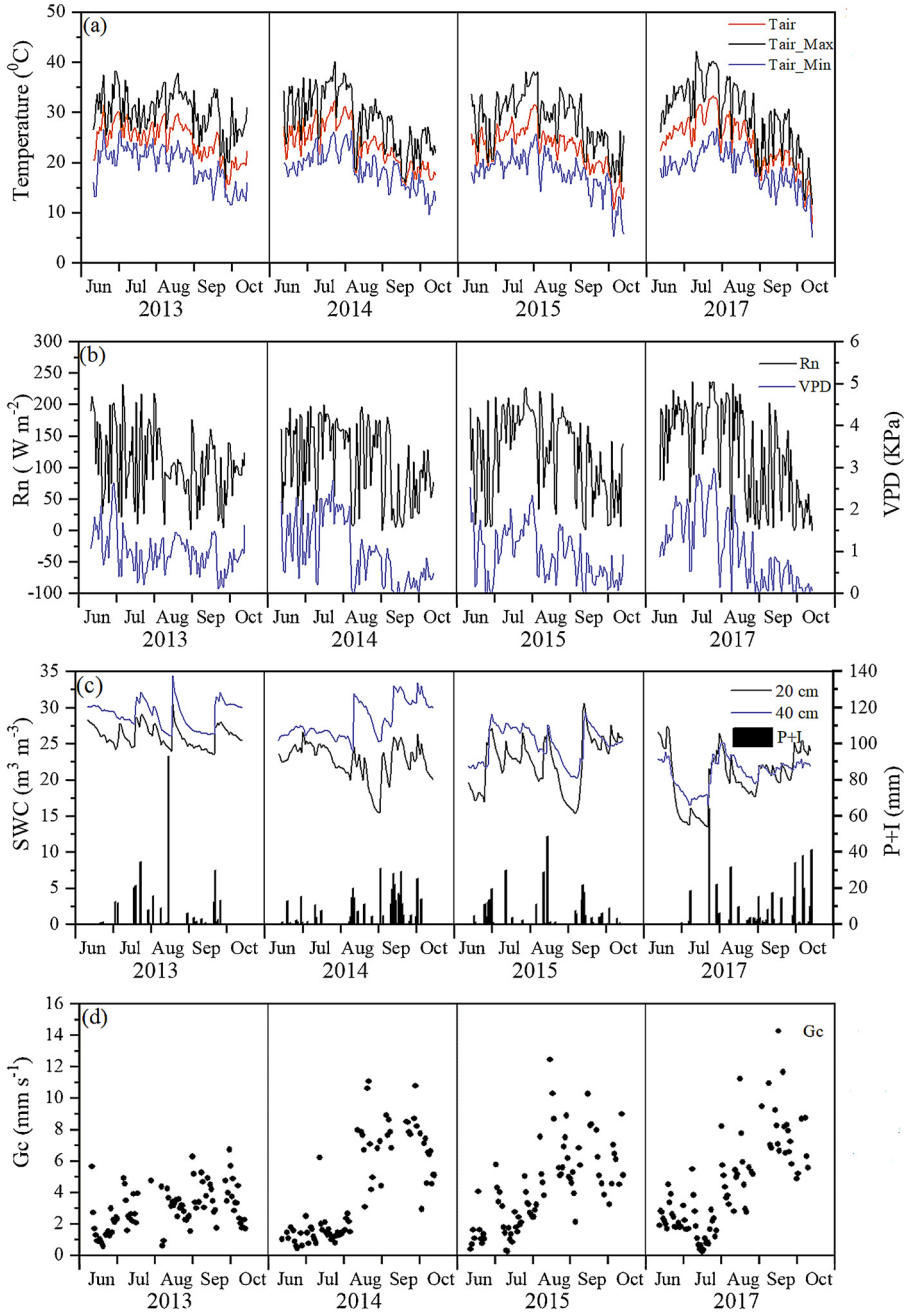

Fig. 2. Seasonal variability of environmental factors in 2013, 2014, 2015, and 2017. (a) Mean daily temperature (T_{air}), maximum daily temperature (T_{air_Max}), and minimum daily temperature (T_{air_Min}). (b) Daily net radiation (R_n) and vapor pressure deficit (*VPD*). (c) Soil water content (*SWC*) and precipitation plus irrigation ($P + I$). (d) Canopy conductance (G_c).

$$G_c = \frac{\gamma \lambda ET G_a}{\Delta(R_n - G) + \rho c_p VPD - LE(\Delta + \gamma)}. \quad (4)$$

The aerodynamic conductance (G_a) was calculated using the equation proposed by Monteith and Unsworth (2007):

$$G_a = \left(\frac{u}{u_*^2} + 6.2u_*^{-2/3}\right)^{-1}, \quad (5)$$

where u is the average wind speed, and u_* is the friction velocity.

2.6. Evapotranspiration partitioning

Unlike many previous studies using sap flow combined with micro lysimeter, we selected a simple and practical method to separate *E* and *T* proposed by Zhou et al. (2016). Although the behavior of stomatal is influenced by environmental factors, the potential water use efficiency (*uWUEp*) at a stomatal scale in an ecosystem with a homogeneous underlying surface is assumed to be nearly constant (Medlyn et al., 2011), and variations of actual water use efficiency (*uWUE*) can be attributed to the soil evaporation (Zhou et al., 2016). Thus, the method can be used to estimate *T* with the measured *ET*, actual *uWUE*, and estimated *uWUEp*. Another assumption of this method is that the ecosystem *T* is equal to *ET* at some growth stages, so *uWUEp* can be estimated using the upper bound of the ratio of $GPP{\cdot}VPD^{0.5}$ to *ET*, where *GPP* is the gross primary production, and *VPD* is the vapor pressure deficit.

Here, we used the method reported by Zhou et al. (2016), which uses the 95th quantile regression between $GPP{\cdot}VPD^{0.5}$ and *ET* to estimate *uWUEp*. Zhou et al. (2016) demonstrated that the 95th quantile regression for *uWUEp* at flux tower sites was consistent with the *uWUE*

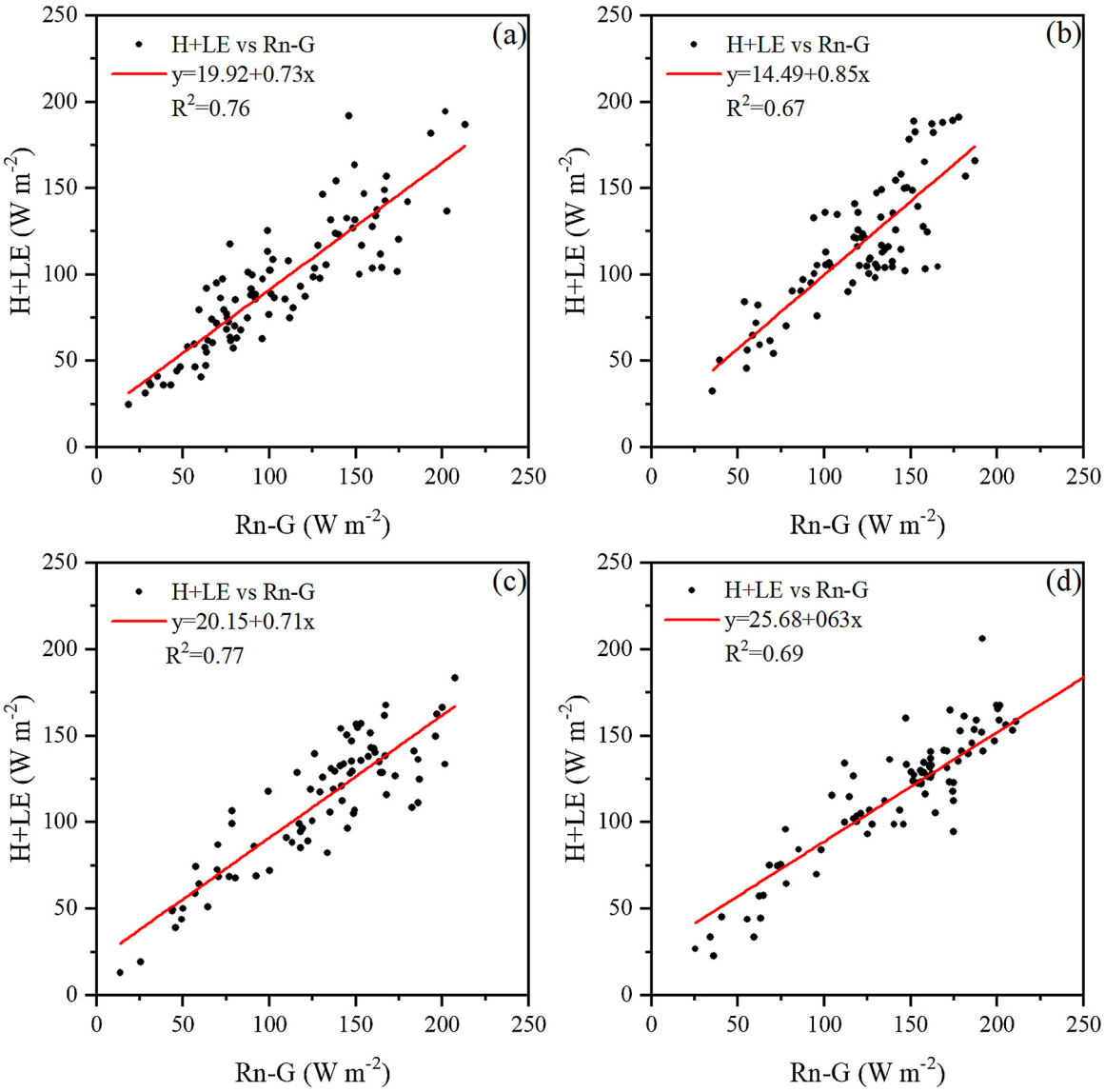

Fig. 3. Regression analysis of energy balance closure in (a) 2013, (b) 2014, (c) 2015, and (d) 2017.

derived at the leaf scale for different ecosystems. In addition, the variability of seasonal and interannual *uWUEp* was relatively small for a homogeneous canopy. Therefore, *T* can be estimated using Eq. (6):

$$\frac{T}{ET} = \frac{uWUE}{uWUE_p} \tag{6}$$

The calculation of *VPD* was based on T_{air} and *RH* data, and the method of gap-filling was the marginal distribution sampling (MDS) method proposed by Reichstein et al. (2005). To calculate *GPP*, the complete series of net ecosystem exchange (*NEE*) was partitioned into *GPP* and respiration (*Re*) using the method proposed by Reichstein et al. (2005). Finally, *ET* was calculated using the latent heat flux and air temperature. Based on *GPP*, *ET*, and *VPD* data, *T* can be calculated using the method proposed by Zhou et al. (2016).

2.7. Statistical analysis

The statistics we used to evaluate the performance of this method were (1) root mean squared deviation (RMSD); (2) relative RMSD (RRMSD); and (3) mean deviation (MD). They can be calculated as follows:

$$RMSD = \sqrt{\frac{1}{n}\sum_{i=1}^{n}(P_i - O_i)^2} \tag{6}$$

$$RRMSD = \frac{RMSD}{O_{average}} \tag{7}$$

$$MD = \frac{1}{n}\sum (P_i - O_i) \tag{8}$$

where P_i is the *i*th predicted value, O_i is the *i*th observed value, $O_{average}$ is the average of the observed values, and *n* is the number of samples.

3. Results and discussion

3.1. Meteorological conditions and energy balance

The variations of climate conditions, soil moisture, and biological factors during the maize growth seasons over four years are shown in Fig. 2, and the average values of these factors for each growth stage are shown in Table 1. As Fig. 1(a) shows, the daily average air temperature ranged from 7.81 °C to 33.30 °C, the daily maximum temperature varied from 11.65 °C to 42.19 °C, and the daily minimum temperature ranged from 5.08 °C to 26.80 °C. Considering different growth stages,

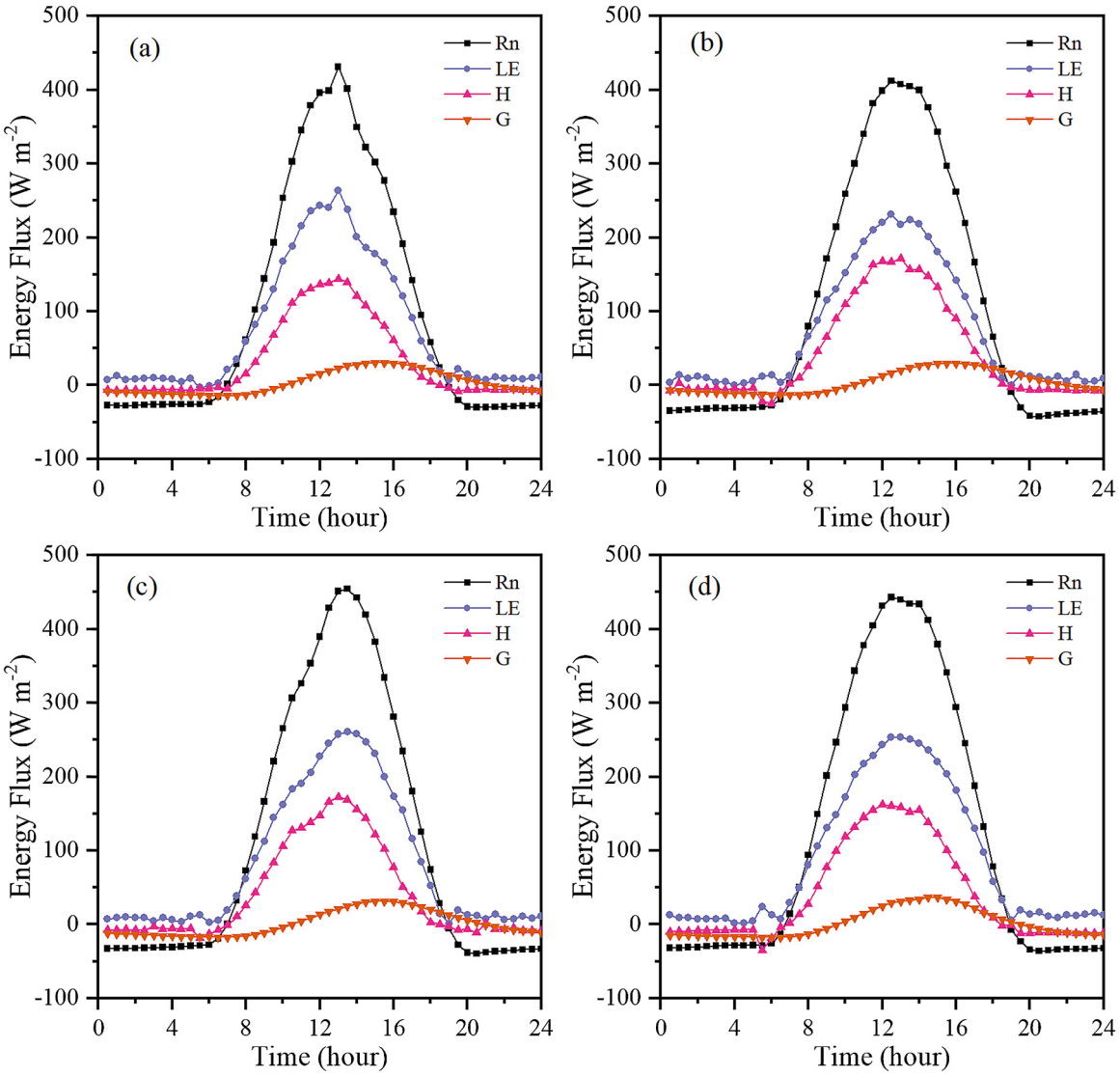

Fig. 4. Diurnal variation of net radiation (R_n), latent heat flux (*LE*), sensible heat flux (*H*), and soil heat flux in (a) 2013, (b) 2014, (c) 2015, and (d) 2017.

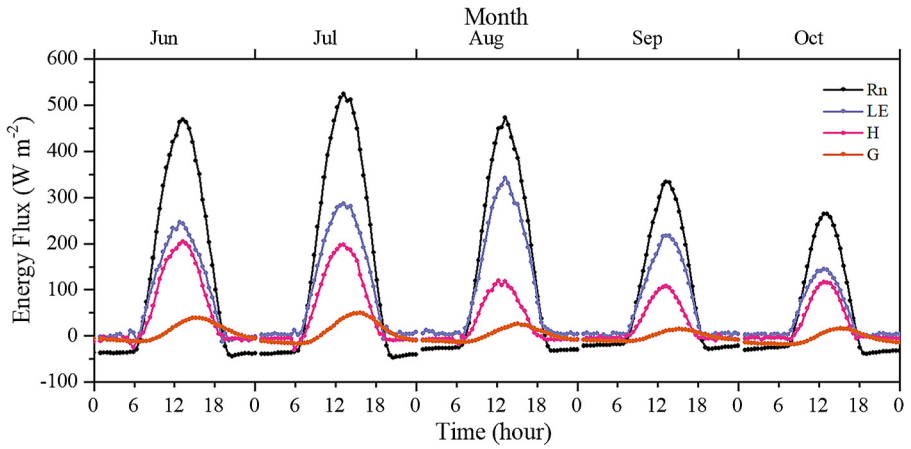

Fig. 5. Monthly averaged diurnal variation of energy components in maize season over four years. R_n is the net radiation; *LE* is the latent heat flux; *H* is the sensible heat flux; *G* is the soil heat flux.

the average air temperatures in the initial and development stages were usually higher than in the mid and late stages. Fig. 2(b) shows the seasonal variation of R_n and *VPD* during maize growing seasons. The seasonal pattern of R_n was similar to *VPD* during maize growing seasons. Daily averaged R_n values were relatively high from early June to August, and peak values of daily average net radiation were about 200 W m^{-2}. Due to the decrease of global radiation, R_n decreased in September–October. Fig. 1(c) exhibits the change of canopy

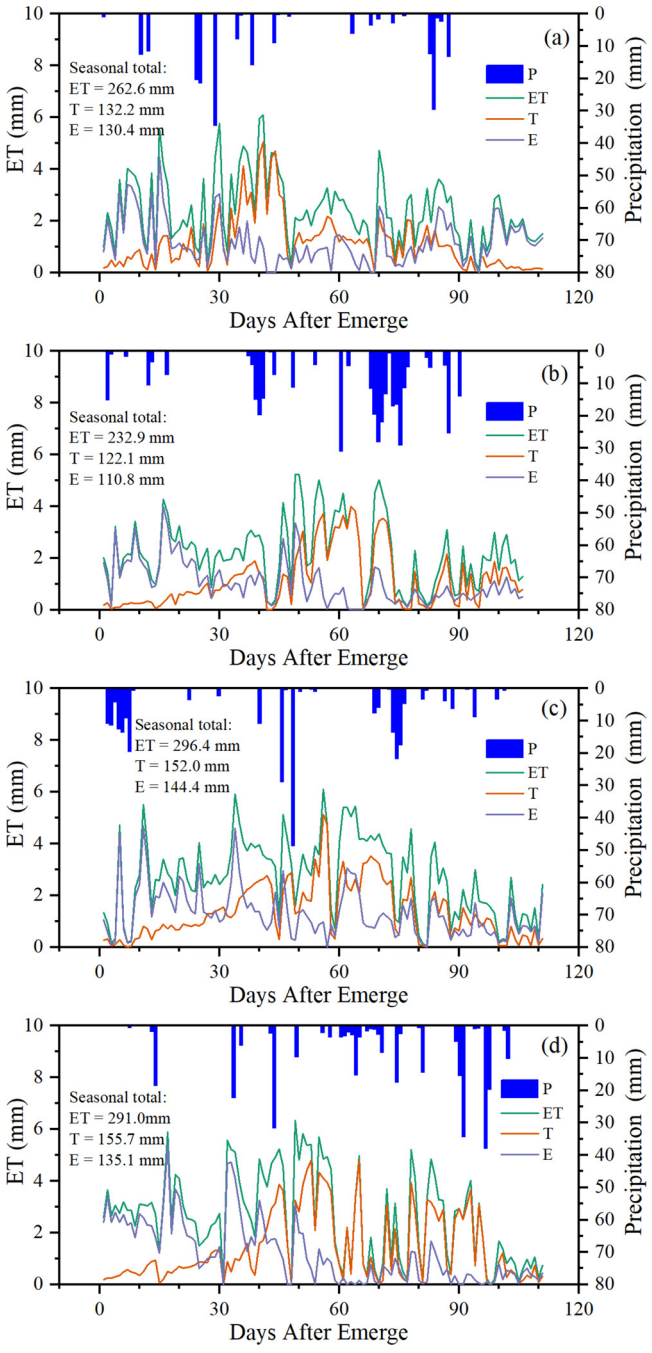

Fig. 6. Seasonal variations of evapotranspiration (*ET*), Transpiration (*T*), and evaporation (*E*) in (a) 2013, (b) 2014, (c) 2015, and (d) 2017.

conductance in four maize growing seasons. Although we only have the observation of soil moisture at shallow surface, it can reflect the root zone moisture as well. Daily averaged soil water content (SWC) was maintained at a high level, and the summer maize rarely suffered water stress during the four-year observation period. G_c ranged from 0 to 2 mm s^{-1} during the initial stages. With the development of the canopy, G_c reached up to 6–10 mm s^{-1} in the mid stage. And it decreased to 5 mm s^{-1} in the late stage because of the senescence of the canopy.

Fig. 3 shows the linear fitting between R_n-G and H + LE. For 2013, 2014, 2015, and 2017, the slopes were 0.73, 0.85, 0.71, and 0.63, the intercepts were 19.92 W m^{-2}, 14.49 W m^{-2}, 20.15 W m^{-2}, and 25.68 W m^{-2}, and the coefficients of determination (R^2) were 0.799, 0.88, 0.77, and 0.69, respectively. The energy balance closure statistics at this area were acceptable compared with the results reported by Wilson et al. (2002), Li (2005), and Foken (2008). To overcome the problem of energy imbalance, the Bowen ratio method was applied to correct the measured *LE*. Based on the corrected long-term reliable observation data, we can calculate K_c and other parameters.

3.2. Diurnal variation of energy fluxes

Fig. 4 shows the daily variation of R_n, *LE*, *H*, and *G* during the four growing seasons (2013, 2014, 2015, and 2017). The monthly and seasonally averaged energy fluxes exhibited a single peak pattern during a day. The R_n was less than zero and rapidly increased in the morning, reaching peak values at 12:30 p.m. to 13:30 p.m.. *LE* and *H* varied with R_n, and the peak values of *LE* were always higher than the peak values of *H*. During the four growing seasons, the average R_n, *LE*, *H*, and *G* ranged from 100.4 W m^{-2} to 120.0 W m^{-2}, 72.6 W m^{-2} to 87.2 W m^{-2}, 32.8 W m^{-2} to 43.1 W m^{-2}, and 1.3 W m^{-2} to 4.0 W m^{-2}, respectively. This indicates that in the maize agroecosystem, there was a larger proportion of R_n transfer to *LE*, and a relatively small proportion of R_n was absorbed by *H*. The peak of *G* had obvious hysteresis compared to other flux components, and the maximum values occurred at 14:30 p.m. to 15:30 p.m.. The results were consistent with the study conducted by Facchi et al. (2013) at a maize cropland in Italy.

Fig. 5 shows the monthly averaged diurnal variation of energy fluxes (R_n, *LE*, *H*, and *G*) during four growing seasons. The variation of energy partitioning shows a clear seasonal pattern. The peak value of R_n (524.2 W m^{-2}) occurred in July, whereas the peak value of *LE* (342.4 W m^{-2}) occurred in August when the leaf area index (*LAI*) reached the maximum value. *G* accounted for a low proportion compared to the other energy components during the whole growing season. *H* was relatively high in June and July because of the low *LAI* and high net radiation. With the canopy developing, more net radiation was partitioned into *LE* rather than *H*. And *H* increased slightly when the maize was harvested.

3.3. Seasonal variation of evapotranspiration, soil evaporation, and transpiration

Table 1 shows the mean values of meteorological factors and water fluxes in different growth stages. Since the *VPD* and *LAI* were relatively high, the average daily *ET* was 2.22–3.45 mm day^{-1} in the development stage, which was the highest among the four growth stages. The ratio of *T* to *ET* ranged from 0.11 to 0.81 during the maize growing seasons. The highest values of *T/ET* usually occurred in the mid stage, and the lowest values occurred in the initial or late stages. Fig. 6 shows the seasonal patterns of daily *ET*, *T*, and *E* during the maize growing seasons in 2013, 2014, 2015, and 2017. Seasonal variations of *ET*, *T*, and *E* showed similar patterns in the observations across four years. At the beginning of the maize growing season, the daily values of *T* were about 0.1 mm day^{-1}. With the *LAI* increasing at the development stage, daily values of *T* increased from 1 to 4 mm day^{-1}. Due to the decrease of solar radiation and the senescence of maize in the late stage, daily values of *T* decreased to less than 1 mm day^{-1}. The daily values of *E* had a contrasting pattern with the daily values of *T*. When *LAI* was low, a large proportion of solar radiation could transfer through the canopy to the soil surface, so the soil evaporation was large compared to the transpiration. With the *LAI* increasing, more radiation was intercepted by the canopy, so the daily values of *E* decreased from around 3 mm day^{-1} to less than 1 mm day^{-1}. Soil evaporation, especially in the initial stage, had large variability after precipitation or irrigation. In the initial stage, soil evaporation accounted for 78 %–85 % of *ET*. With the development of the canopy, the proportion of soil evaporation in *ET* decreased gradually in the development stage. In the mid growing stage, the soil evaporation was very small, and the transpiration accounted for 54 %–81 % of *ET*. When the maize entered the late stage, the variation in soil evaporation was large, and the ratio of *E* to *ET* ranged from 39 % to 89 %. *ET* totals in 2013, 2014, 2015, and 2017

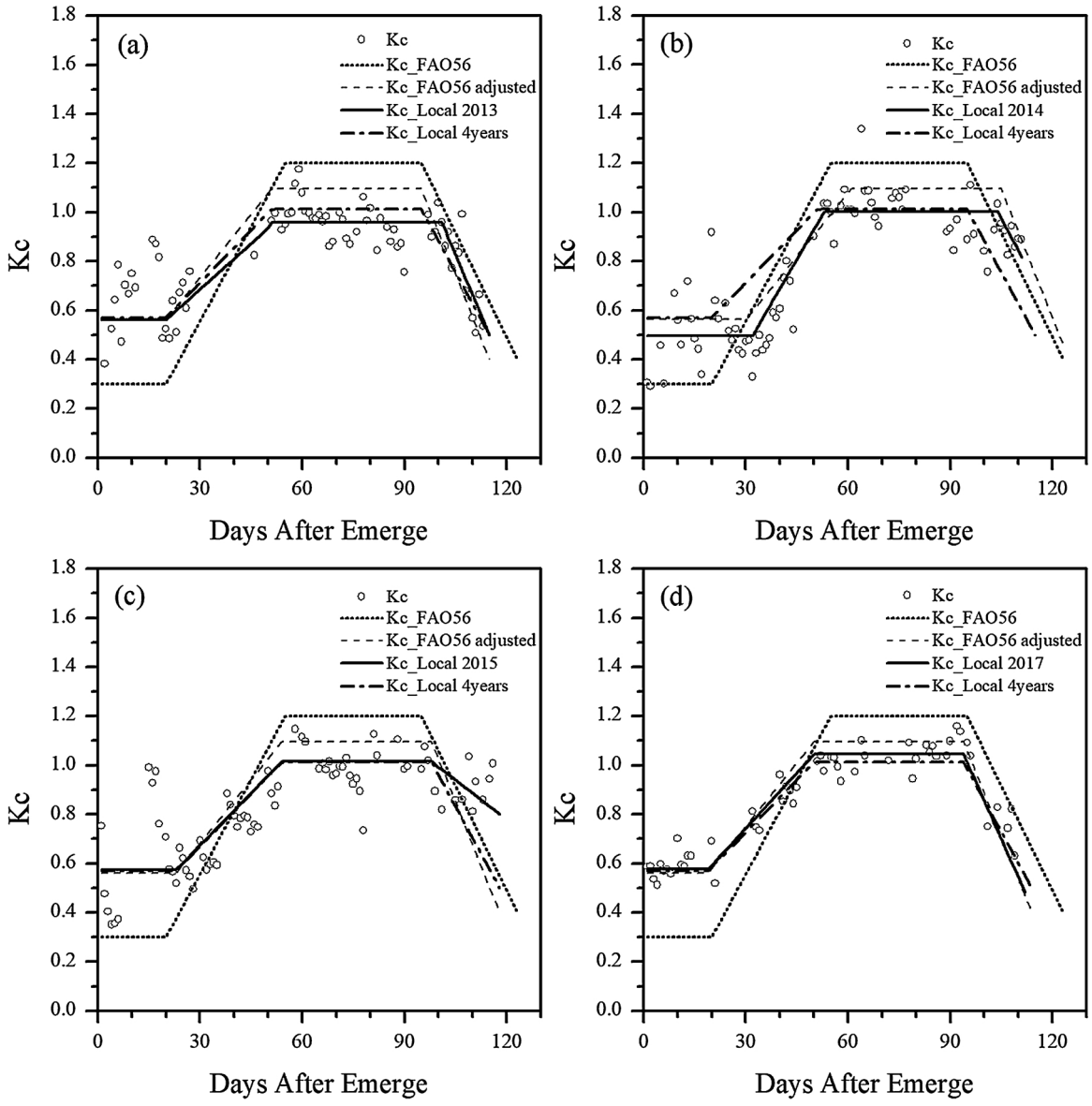

Fig. 7. K_c values derived from the experimental data (black dots), the FAO-56 standard curve (the short dot line), the FAO-56 adjusted curve (the dash line), the locally developed K_c curves based on one year of data (the solid lines), and the locally developed K_c curves based on four years of data (the dash dot lines). (a) 2013, (b) 2014, (c) 2015, (d) 2017.

Table 3
Locally developed crop coefficient (*Kc*) in Yangling, China.

Crop coefficient	FAO-56 standard	FAO-56 adjusted	2013	2014	2015	2017	4-years
Kc ini	0.30	0.56	0.56	0.49	0.64	0.58	0.57
Kc mid	1.20	1.10	0.96	1.02	1.01	1.04	1.01
Kc lat	0.30	0.40	0.56	0.81	0.82	0.48	0.50

were 262.6 mm, 232.9 mm, 296.4 mm, and 291.0 mm, respectively. The ratios of *T* to *ET* (*T/ET*) were 50.3 %, 52.4 %, 51.3 %, and 53.5 % for 2013, 2014, 2015, and 2017, respectively. These values indicate that plant transpiration and soil evaporation account for a comparable proportion of evapotranspiration. The ratios of *E* to *ET* observed in this study were slightly higher than the ratios (36 %–47.2 %) observed by Gong et al. (2017) in conventional flat cultivation without mulching.

3.4. Single and dual crop coefficients

The reference duration of the growth stages for summer maize proposed by FAO-56 and the actual lengths of growth stages during the observation period are shown in Table 1. The lengths of stages in the standard curves referred to the values provided by FAO56, while the lengths of stages in the adjusted curves and locally developed curves were observed in the field. Missing data in the daily K_c datasets were caused by instruments malfunctioning and bad weather conditions. As Fig. 5 shows, the daily soil evaporation in the initial stage sharply increased after rainfall or irrigation events. These unreliable values were removed when calculating $K_{c\text{-}ini}$. Other daily K_c values were used when calculating K_c curves, although irrigation and intense precipitation also caused changes in K_c due to high soil evaporation.

Fig. 7 shows the daily K_c values calculated using observed data (black dots), the FAO-56 reference curve (the short dot line), the FAO-56 adjusted curve (the dashed line), the locally developed K_c curves using one year of data (the solid lines), and the locally developed K_c curves using four years of data (the dash-dot lines). With the *LAI*

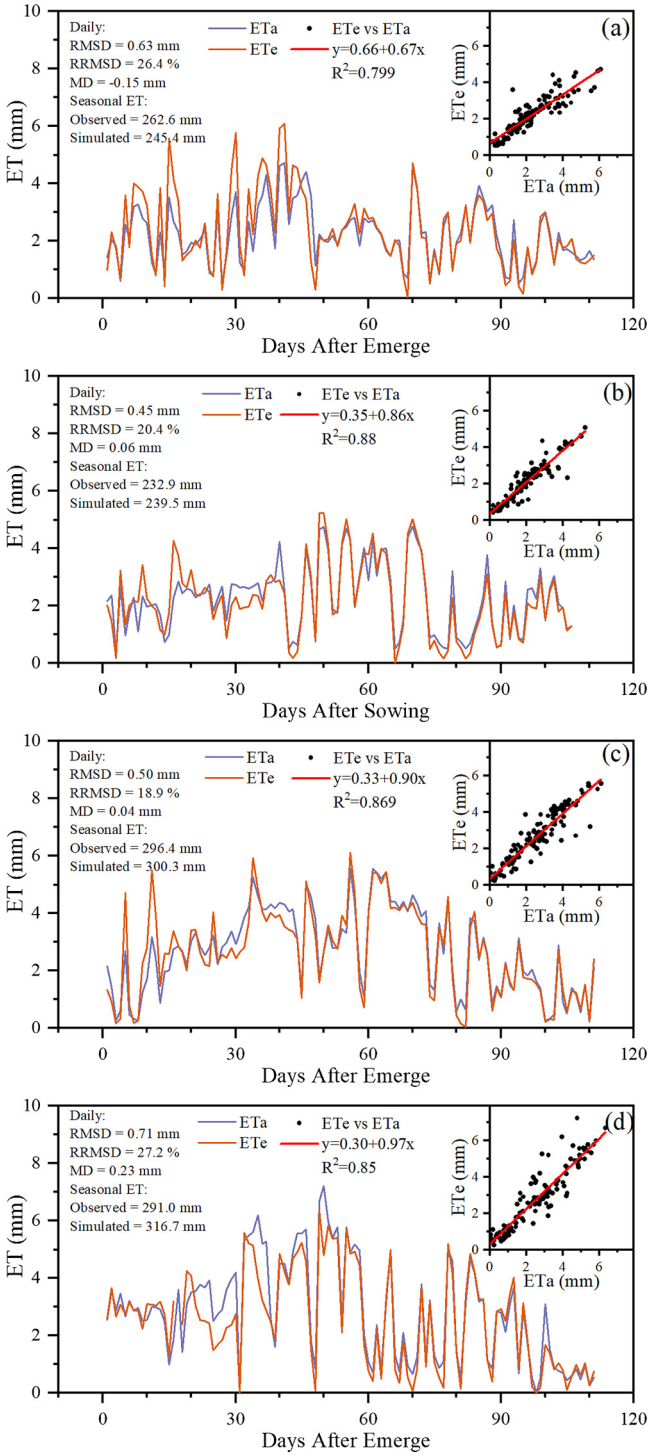

Fig. 8. Comparison between measured ET and simulated ET using crop coefficient in (a) 2013, (b) 2014, (c) 2015, and (d) 2017.

increasing, the daily K_c increased from 0.57 to 1.01. The daily K_c stayed at 1.01 in the mid stage and decreased gradually in the late stage because of the senescence of maize. Based on the daily K_c calculated by the ratio of ET_c to ET_0, we developed local K_c curves to accurately estimate the crop water requirement. The locally derived K_c values in the initial stage (0.49–0.64) were generally higher than the values (0.35) provided by FAO56 and consistent with the adjusted K_c (0.56) based on the local climate. For the K_c in the mid stage, the locally derived K_c was lower than the standard values and the adjusted value in FAO56. The variability of K_c in the late stage was very large. The locally derived K_c in the late stage using one-year data ranged from 0.48 to 0.82, depending on the soil moisture and the grain moisture when harvested. The variability of the locally derived $K_{c\text{-}mid}$ based on the one-year dataset was small, and the K_c values derived from the one-year dataset were comparable with the $K_{c\text{-}mid}$ values derived from the four-year dataset. (Table 3)

Fig. 8 shows the seasonal variation of estimated and measured *ET* as well as the linear regression analysis between measured *ET* (ET_a) and estimated *ET* (ET_e). For four growing seasons, the RMSD ranged from 0.45 mm to 0.68 mm; the RRMSD ranged from 18.9 % to 26.4 %; the MD ranged from 0.04 mm to 0.25 mm; and the R^2 ranged from 79.9 % to 88 %. In total, the estimated *ET* was slightly greater than the observed value except in 2013. This indicates that the crop coefficient method can provide a good prediction of daily *ET*. Therefore, we can use the locally derived K_c curve to guide the irrigation strategy. The highest differences between estimated *ET* and measured *ET* usually occurred before the mid stage, which was related to the variation of soil evaporation after precipitation or irrigation. Moreover, the K_c curve cannot characterize the *ET* in the initial and development stages as accurately as in the mid and late stages.

Fig. 9 shows the basal crop coefficient (K_{cb}*K_s) and soil evaporation (K_e) of maize. The basal crop coefficient (K_{cb}*K_s) of summer maize showed a similar pattern as K_c and plant transpiration, but the magnitudes of K_{cb}*K_s were lower than K_c. K_{cb}*K_s values ranged from nearly 0 to 0.9. The maximum values usually occurred around 60 days after emergence (DAE 60 In the early and rapid growth stages, K_{cb}*K_s gradually increased from 0.5 to 0.9 as the canopy developed. In the mid stage, K_{cb}*K_s ranged with great variability from 0.4 to 0.9, which was lower than the values reported in other literature. Reported mid-season K_{cb} values of maize were 1.05 (Rosa et al., 2012), 1.10 (Zhao et al., 2013), 1.12 (Martins et al., 2013), and 1.15 (Zhang et al., 2013). In the late stage, K_{cb}*K_s linearly decreased from 0.5 to 0.2. The four-year averaged soil evaporation coefficient (K_e) of summer maize decreased with increasing *LAI* and land cover from DAE 0 to DAE 75 (Fig. 8). Peak values of K_e decreased from around 0.7 to around 0.2 with increasing DAE. With the maize approaching maturity, K_e increased from around 0.2 to around 0.7. The variability of K_e was greater than K_{cb}*K_s. The reason is that soil evaporation is more sensitive to surface moisture than plant transpiration.

Maize growth and senescence rates vary with maize variety, weather, soil nutrition level, and field management practice. The most vital aspect of developing appropriate crop coefficient values is the phenology. The largest seasonal weather effect on plant growth in temperate climates is during the early season when low air and soil temperatures may delay crop growth by several days. Therefore, developing K_{cb} values based on growing degree day (GDD) rather than DAE would further improve K_{cb} estimates.

4. Discussion

4.1. Effects of physiological and meteorology factors on K_c

Fig. 10 displays the nonlinear curve fitting between K_c and canopy conductance (G_c). The relationships between K_c and G_c were statistically significant during four seasons (the determination coefficients were 0.63, 0.92, 0.82, and 0.75). K_c increased rapidly when G_c increased from 0 to 6 mm^{-1}, indicating that the biological factor is the primary factor in determining the crop coefficient, but K_c was insensitive when G_c exceeded 6 mm^{-1}. Ding et al. (2015) reported a similar relationship between G_c and K_c for a spring maize field in Northwest China. In addition, we analyzed the relationship between K_c and *LAI*, but the *LAI* cannot explain as much variability in *ET* as G_c. This finding contrasts with some studies which found that *LAI* can explain more variability of K_c than G_c. Because the variability of soil evaporation was high, the relationship between *LAI* and K_c was not as significant as *Gc*. Xu et al. (2018) also reported that the canopy size can

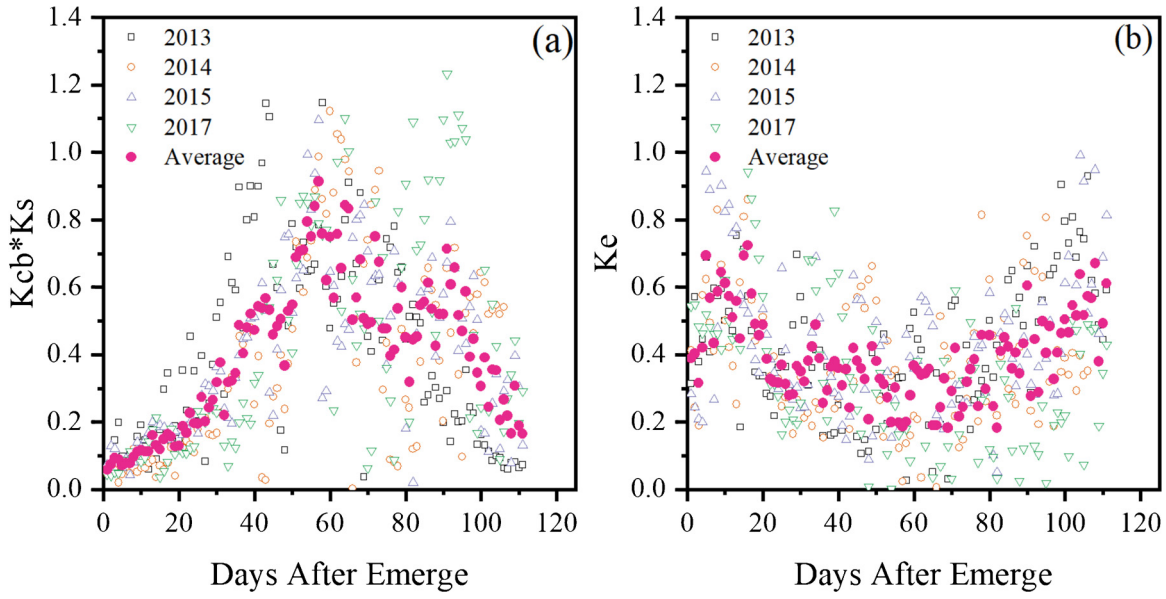

Fig. 9. (a) Basal crop coefficient and stress coefficient (K_{cb}*K_s) from summer maize in 2013, 2014, 2015, 2017, and the four-year average. (b) Soil evaporation coefficients (K_e) from summer maize in 2013, 2014, 2015, 2017, and the four-year average.

significantly affect the crop coefficient, with larger canopy sizes leading to higher crop coefficients.

4.2. Variation of the maize K_c in different regions

A review of locally developed $K_{c\text{-}mid}$ of maize in other regions, the location of the study area, climate type, and the instrument used to measure *ET* are included in Table 4. Most of the $K_{c\text{-}mid}$ values calculated using the data measured by lysimeter are higher than those calculated using the data measured by EC systems. Due to a limited representative area, lysimeters are prone to overestimating *ET* compared with other instruments (Rana and Katerji, 2000; Alfieri et al., 2012). Although EC systems may underestimate *ET* because of flaws with their energy balance closure, EC systems can accurately capture *ET* information over short-term periods in large areas. The calculated $K_{c\text{-}mid}$ of this study was consistent with the $K_{c\text{-}mid}$ reported in Shouyang, Shanxi (Gong et al., 2017), Nebraska, USA (Suyker and Verma, 2009), and Landriano, Italy (Facchi et al., 2013) and was slightly higher than the $K_{c\text{-}mid}$ of maize planted at Hexi corridor (Ji et al., 2017). However, the $K_{c\text{-}mid}$ in this area was much lower than the results reported by Li et al. (2008) in Wuwei, China, and by Payero and Irmak (2011) in North Platte, Nebraska, USA, using EC systems. It was also slightly lower than the $K_{c\text{-}mid}$ reported by Zhao et al. (2010) in Pingchuan, China, using the Bowen Ratio Energy Balance (BREB) system. Although Parkes et al. (2005) and Kang et al. (2003) proposed a K_c value of maize in this area, they used the lysimeter method to measure the actual *ET*. Moreover, due to the variety of updated and improved farming practices and climate change, it is necessary to use a more precise method to determine the crop coefficient. Using the eddy covariance method, the calculated K_c was significantly lower than the results reported by Parkes et al. (2005) and Kang et al. (2003). It was also lower than the K_c values in studies conducted in Uvalde, TX, USA (Piccinni et al., 2009), Luancheng, China (Liu et al., 2002), Naiman, China (Li et al., 2003), Beijing, China (Xu et al., 2018), Fars, Iran (Shahrokhnia and Sepaskhah, 2013), Bushland, TX, USA (Howell et al., 2006), and Karnal, India (Tyagi et al., 2003), which used lysimeter *ET* data to derive K_c. In addition, using the soil water balance method, Djaman & Irmak reported that the locally developed $K_{c\text{-}mid}$ in North Platte was 1.08–1.26. According to the discussion, the calculated K_c not only varies with the climate but is also affected by the *ET* measurement method. Sometimes the variability caused by the method of *ET* measurement is more significant than the variability caused by climate conditions.

5. Conclusion

Based on a four-year observation period using an EC system, we derived the local crop coefficient curve and studied evapotranspiration partitioning in a summer maize cropland. Due to the imbalance of energy, we corrected *LE* data before we calculated the actual *ET*. Both energy partitioning and evapotranspiration partitioning have significant seasonal variability. R_n was mainly consumed by *H* during the initial and late stages, whereas R_n was mainly absorbed by water vapor and transferred into latent heat during the development and mid stages. In the initial stage, soil evaporation accounted for 78 %–85 % of the *ET*. With the development of the canopy, the proportion of soil evaporation in *ET* decreased gradually. In the mid growing stage, the soil evaporation was very small, and the transpiration accounted for 54 %–81 % of the *ET*. The crop coefficients derived by local datasets were 0.57, 1.01, and 0.50 in the initial, mid, and late stages, respectively. The locally developed K_c curve can provide a good prediction of the crop water requirement. The variability in crop coefficient at different regions was high, which was attributed to the differences in climate and measurement methods. Different measurement methods can result in great variability of the crop coefficient. The K_c calculated using *ET* datasets from lysimeter measurements ranged from 1.20 to 1.53, which was significantly higher than the K_c calculated using EC datasets. Although lysimeters are widely used as a standard method to measure *ET*, lysimeters commonly overestimate K_c and crop evapotranspiration due to their limited representative area.

Declaration of Competing Interest

The authors declare that they have no known competing financial interests or personal relationships that could have appeared to influence the work reported in this paper.

Acknowledgments

This work was supported by the National Natural Science Foundation of China (51879223) and the National Key Research and Development Program of China (2016YFC0400200) and 111 Project (B12007).

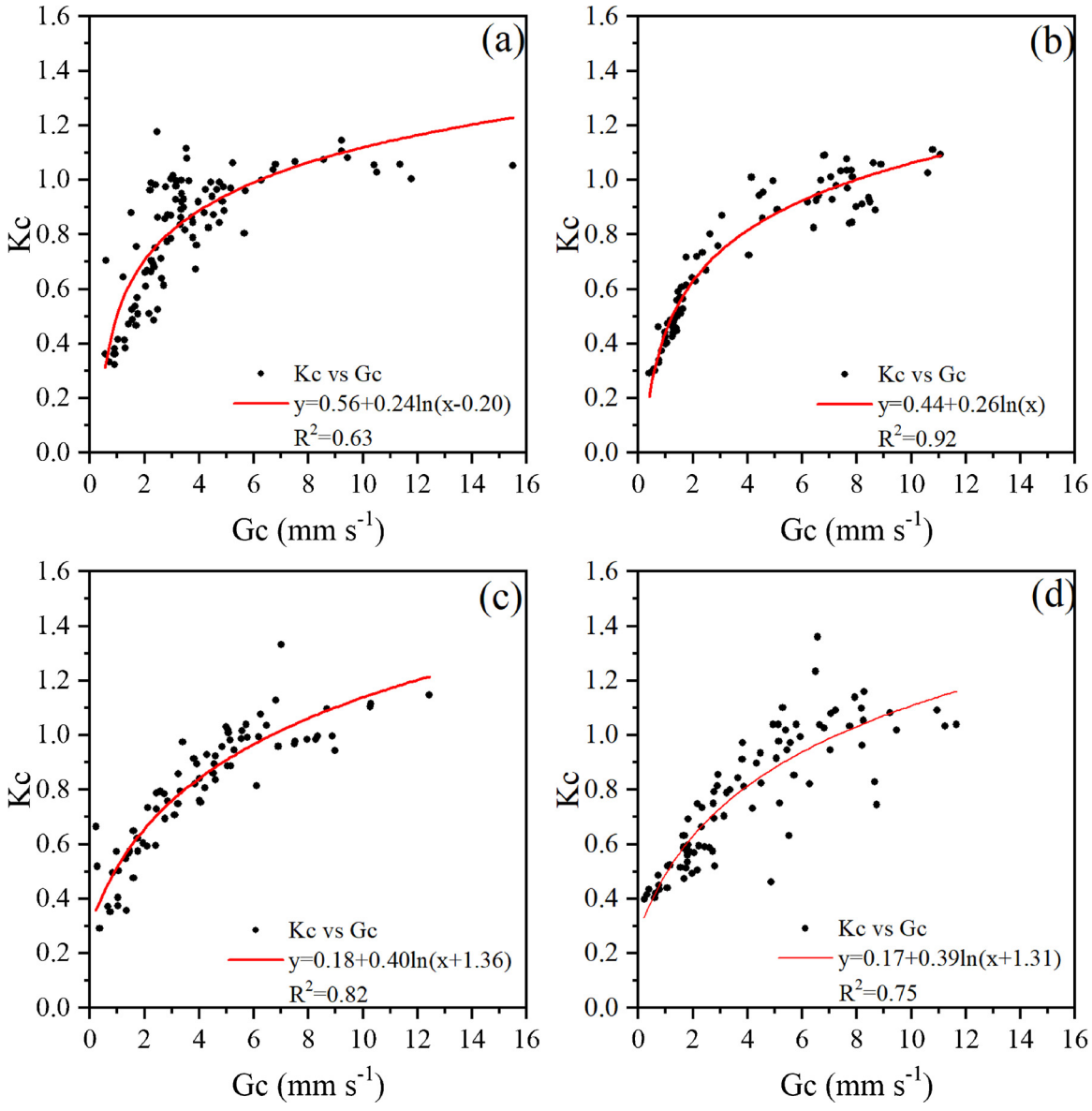

Fig. 10. The relationship between daily crop coefficient (K_c) and canopy conductance (G_c) in (a) 2013, (b) 2014, (c) 2015, and (d) 2017.

Table 4
Comparison of locally developed crop coefficient (*Kc*) for maize in other regions under different climate.

Site	Climate	Measurement method	Local Kc-mid	References
Yangling, Shaanxi, China (34°17′N, 108°04′E, 521 m a.s.l.)	Dry semi-humid	Eddy covariance	1.00 ± 0.04	This study
Shouyang, Shanxi (37°45′N, 113°12′E, 1202 m a.s.l.)	Semi-arid	Eddy covariance	1.01 ± 0.05	Gong et al. (2017)
Hexi Corridor, China (39°19′N, 100°08′E, 1365 m a.s.l.)	Arid	Eddy covariance	0.88–0.93	Ji et al. (2017)
Landriano, Italy (45°19′N, 9°15′E, 88 m a.s.l.)	Humid	Eddy covariance	0.99	Facchi et al. (2013)
Wuwei, Gansu, China (37°85′N, 102°85′E, 1581 m a.s.l.)	Arid	Eddy covariance	1.39–1.46	Li et al. (2008)
Nebraska, USA (41°09′N, 96°28′W, 361 m a.s.l.)	Semi-arid	Eddy covariance	1.03 ± 0.07	Suyker and Verma (2009)
North Platte, Nebraska, USA (41°6′N, 100°48′W, 861 m a.s.l.)	Semi-arid	Eddy covariance	1.25	Payero and Irmak (2011)
Yangling, Shaanxi, China (34°17′N, 108°04′E, 521 m a.s.l.)	Dry semi-humid	Lysimeter	1.25	Parkes et al. (2005)
Yangling, Shaanxi, China (34°17′N, 108°04′E, 521 m a.s.l.)	Dry semi-humid	Lysimeter	1.43	Kang et al. (2003)
Luancheng, Shandong, Hebei (37°50′N, 114°40′E, 50 m a.s.l.)	Semi-humid	Lysimeter	1.38	Liu et al. (2002)
Uvalde, TX, USA (29°13′ N, 99°45′ W; 283 m a.s.l.)	Semi-arid	Lysimeter	1.2	Piccinni et al. (2009)
Naiman, Inner Mongolia, China (42°58′ N, 120°43′ E; 345 m a.s.l.)	Semi-arid	Lysimeter	1.26	Li et al. (2003)
Beijing, China (40°17′N, 116°39′E, 50 m a.s.l.)	Semi-humid	Lysimeter	1.53–1.40	Xu et al. (2018)
Kooshkak, Fars, Iran (30°4′N, 52°35′E, 1620 m a.s.l.)	Arid	Lysimeter	1.40	Shahrokhnia and Sepaskhah (2013)
Bushland, TX, USA (35°11′N, 102°06′W, 1170 m a.s.l.)	Semi-arid	Lysimeter	1.17	Howell et al. (2006),
Karnal, India (29°43′N, 76°58′E, 1170 m a.s.l.)	Semi-arid	Lysimeter	1.23	Tyagi et al. (2003)
Pingchuan, Gansu, China (39°24′N, 100°10′E, 1549 m a.s.l.)	Arid	Bowen Ratio Energy Balance	1.15	Zhao et al. (2010)
North Platte, Nebraska, USA (40°43′N, 98°8′W, 552 m a.s.l.)	Semi-arid	Soil water balance	1.08–1.26	Djaman and Irmak (2013)

Appendix A. Supplementary data

Supplementary material related to this article can be found, in the online version, at doi:https://doi.org/10.1016/j.agwat.2020.106164.

References

Alfieri, J.G., Kustas, W.P., Prueger, J.H., Hipps, L.E., Evett, S.R., Basara, J.B., Neale, C.M.U., French, A.N., Colaizzi, P., Agam, N., Cosh, M.H., Chavez, J.L., Howell, T.A., 2012. On the discrepancy between eddy covariance and lysimetry-based surface flux measurements under strongly advective conditions. Adv. Water Resour. 50, 62–78. https://doi.org/10.1016/j.advwatres.2012.07.008.

Allen, R.G., Pereira, L.S., Raes, D., Smith, M., 1998. Crop Evapotranspiration-Guidelines for Computing Crop Water Requirements-FAO Irrigation and Drainage Paper 56. FAO, Rome, pp. D05109 300.

Allen, R.G., Pereira, L.S., Howell, T.A., Jensen, M.E., 2011. Evapotranspiration information reporting: I. Factors governing measurement accuracy. Agric. Water Manage. 98, 899–920. https://doi.org/10.1016/j.agwat.2010.12.015.

ASCE-EWRI, 2005. The ASCE Standardized Reference Evapotranspiration Equation. Technical Committee Rep. to the Environmental and Water Resources Institute of ASCE from the Task Committee on Standardization of Reference Evapotranspiration.

Baldocchi, D.D., 2003. Assessing the eddy covariance technique for evaluating carbon dioxide exchange rates of ecosystems: past, present and future. Glob. Change Biol. 9, 479–492. https://doi.org/10.1046/j.1365-2486.2003.00629.x.

Ding, R., Tong, L., Li, F., Zhang, Y., Hao, X., Kang, S., 2015. Variations of crop coefficient and its influencing factors in an arid advective cropland of northwest China. Hydrol. Process. 29, 239–249. https://doi.org/10.1002/hyp.10146.

Djaman, K., Irmak, S., 2013. Actual crop evapotranspiration and alfalfa- and grass-reference crop coefficients of maize under full and limited irrigation and rainfed conditions. J. Irrig. Drain. Eng. 139, 433–446. https://doi.org/10.1061/(ASCE)IR.1943-4774.0000559.

Facchi, A., Gharsallah, O., Corbari, C., Masseroni, D., Mancini, M., Gandolfi, C., 2013. Determination of maize crop coefficients in humid climate regime using the eddy covariance technique. Agric. Water Manage. 130, 131–141. https://doi.org/10.1016/j.agwat.2013.08.014.

Falge, E., Baldocchi, D., Olson, R., Anthoni, P., Aubinet, M., Bernhofer, C., Burba, G., Ceulemans, R., Clement, R., Dolman, H., 2001. Gap filling strategies for defensible annual sums of net ecosystem exchange. Agric. For. Meteorol. 107, 43–69. https://doi.org/10.1016/j.agrformet.2006.03.003.

Foken, T., 2008. The energy balance closure problem: an overview. Ecol. Appl. 18, 1351–1367. https://doi.org/10.1890/06-0922.1.

Gong, D., Mei, X., Hao, W., Wang, H., Caylor, K.K., 2017. Comparison of ET partitioning and crop coefficients between partial plastic mulched and non-mulched maize fields. Agric. Water Manage. 181, 23–34. https://doi.org/10.1016/j.agwat.2016.11.016.

Howell, T.A., Evett, S.R., Tolk, J.A., Copeland, K.S., Dusek, D.A., Colaizzi, P.D., 2006. Crop coefficients developed at Bushland, Texas for corn, wheat, sorghum, soybean, cotton, and alfalfa. In: World Environmental and Water Resource Congress 2006. Presented at the World Environmental and Water Resources Congress 2006, American Society of Civil Engineers. Omaha, Nebraska, United States. pp. 1–9. https://doi.org/10.1061/40856(200)260.

Ji, X., Chen, J., Zhao, W., Kang, E., Jin, B., Xu, S., 2017. Comparison of hourly and daily Penman-Monteith grass-and alfalfa-reference evapotranspiration equations and crop coefficients for maize under arid climatic conditions. Agric. Water Manage. 192, 1–11. https://doi.org/10.1016/j.agwat.2016.11.016.

Kang, S., Gu, B., Du, T., Zhang, J., 2003. Crop coefficient and ratio of transpiration to evapotranspiration of winter wheat and maize in a semi-humid region. Agric. Water Manage. 59, 239–254. https://doi.org/10.1016/S0378-3774(02)00150-6.

Li, Z., 2005. Energy balance closure at ChinaFLUX sites. Sci. China Earth Sci. 48, 51–62.

Li, Y.-L., Cui, J.-Y., Zhang, T.-H., Zhao, H.-L., 2003. Measurement of evapotranspiration of irrigated spring wheat and maize in a semi-arid region of north China. Agric. Water Manage. 61, 1–12. https://doi.org/10.1016/S0378-3774(02)00177-4.

Li, S., Kang, S., Li, F., Zhang, L., 2008. Evapotranspiration and crop coefficient of spring maize with plastic mulch using eddy covariance in northwest China. Agric. Water Manage. 95, 1214–1222. https://doi.org/10.1016/j.agwat.2008.04.014.

Li, S., Li, S., Li, Y., Li, X., Tian, X., Zhao, A., Wang, S., Wang, S., Shi, J., 2016. Effect of straw management on carbon sequestration and grain production in a maize maize–wheat cropping system in Anthrosol of the Guanzhong Plain. Soil Tillage Res. 157, 43–51. https://doi.org/10.1016/j.still.2015.11.002.

Liu, C., Zhang, X., Zhang, Y., 2002. Determination of daily evaporation and evapotranspiration of winter wheat and maize by large-scale weighing lysimeter and micro-lysimeter. Agric. For. Meteorol. 111, 109–120. https://doi.org/10.1016/s0168-1923(02)00015-1.

Martins, J.D., Rodrigues, G.C., Paredes, P., Carlesso, R., Oliveira, Z.B., Knies, A.E., et al., 2013. Dual crop coefficients for maize in southern Brazil: model testing for sprinkler and drip irrigation and mulched soil. Biosyst. Eng. 115 (3), 291–310. https://doi.org/10.1016/j.biosystemseng.2013.03.016.

Medlyn, B.E., Duursma, R.A., Eamus, D., Ellsworth, D.S., Prentice, I.C., Barton, C.V., Crous, K.Y., De Angelis, P., Freeman, M., Wingate, L., 2011. Reconciling the optimal and empirical approaches to modelling stomatal conductance. Glob. Change Biol. 17, 2134–2144. https://doi.org/10.1111/j.1365-2486.2010.02375.x.

Monteith, J., Unsworth, M., 2007. Principles of Environmental Physics. Academic Press.

Parkes, M., Jian, W., Knowles, R., 2005. Peak crop coefficient values for Shaanxi, Northwest China. Agric. Water Manage. 73, 149–168. https://doi.org/10.1016/j.agwat.2004.10.002.

Payero, J.O., Irmak, S., 2011. Daily crop evapotranspiration, crop coefficient and energy balance components of a surface-irrigated maize field. Evapotranspiration-From Measurements to Agricultural and Environmental Applications. IntechOpen.

Piccinni, G., Ko, J., Marek, T., Howell, T., 2009. Determination of growth-stage-specific crop coefficients (K_c) of maize and sorghum. Agric. Water Manage. 96, 1698–1704. https://doi.org/10.1016/j.agwat.2009.06.024.

Rana, G., Katerji, N., 2000. Measurement and estimation of actual evapotranspiration in the field under Mediterranean climate: a review. Eur. J. Agron. 13, 125–153. https://doi.org/10.1016/s1161-0301(00)00070-8.

Reichstein, M., Falge, E., Baldocchi, D., Papale, D., Aubinet, M., Berbigier, P., Bernhofer, C., Buchmann, N., Gilmanov, T., Granier, A., 2005. On the separation of net ecosystem exchange into assimilation and ecosystem respiration: review and improved algorithm. Glob. Change Biol. 11, 1424–1439. https://doi.org/10.1111/j.1365-2486.2005.001002.x.

Rosa, R.D., Paredes, P., Rodrigues, G.C., Fernando, R.M., Alves, I., Pereira, L.S., Allen, R.G., 2012. Implementing the dual crop coefficient approach in interactive software: 2. Model testing. Agric. Water Manage. 103, 62–77. https://doi.org/10.1016/j.agwat.2011.10.018.

Sánchez, J., LC3pez-Urrea, R., Rubio, E., GonzC!lez-Piqueras, J., Caselles, V., 2014. Assessing crop coefficients of sunflower and canola using two-source energy balance and thermal radiometry. Agric. Water Manage. 137, 23–29. https://doi.org/10.1016/j.agwat.2014.02.002.

Shahrokhnia, M.H., Sepaskhah, A.R., 2013. Single and dual crop coefficients and crop evapotranspiration for wheat and maize in a semi-arid region. Theor. Appl. Climatol. 114, 495–510. https://doi.org/10.1007/s00704-013-0848-6.

Sun, H., Shao, L., Liu, X., Miao, W., Chen, S., Zhang, X., 2012. Determination of water consumption and the water-saving potential of three mulching methods in a jujube orchard. Eur. J. Agron. 43, 87–95. https://doi.org/10.1016/j.eja.2012.05.007.

Suyker, A.E., Verma, S.B., 2009. Evapotranspiration of irrigated and rainfed maize–soybean cropping systems. Agric. For. Meteorol. 149, 0–452. https://doi.org/10.1016/j.agrformet.2008.09.010.

Twine, T.E., Kustas, W.P., Norman, J.M., Cook, D.R., Houser, P.R., Meyers, T.P., Prueger, J.H., Starks, P.J., Wesely, M.L., 2000. Correcting eddy-covariance flux underestimates over a grassland. Agric. For. Meteorol. 103, 279–300. https://doi.org/10.1016/S0168-1923(00)00123-4.

Tyagi, N.K., Sharma, D.K., Luthra, S.K., 2003. Determination of evapotranspiration for maize and berseem clover. Irrig. Sci. 21 (4), 173–181. https://doi.org/10.1007/s00271-002-0061-3.

Wang, S., Zhu, G., Xia, D., Ma, J., Han, T., Ma, T., Zhang, K., Shang, S., 2019. The characteristics of evapotranspiration and crop coefficients of an irrigated vineyard in arid Northwest China. Agric. Water Manage. 212, 388–398. https://doi.org/10.1016/j.agwat.2018.09.023.

Webb, E.K., Pearman, G.I., Leuning, R., 1980. Correction of flux measurements for density effects due to heat and water vapour transfer. Q. J. R. Meteorol. Soc. 106, 85–100. https://doi.org/10.1256/smsqj.44706.

Wilczak, J.M., Oncley, S.P., Stage, S.A., 2001. Sonic anemometer tilt correction algorithms. Bound-Layer Meteorol. 99, 127–150. https://doi.org/10.1023/a:1018966204465.

Wilson, K., Goldstein, A., Falge, E., Aubinet, M., Baldocchi, D., Berbigier, P., Bernhofer, C., Ceulemans, R., Dolman, H., Field, C., 2002. Energy balance closure at FLUXNET sites. Agric. For. Meteorol. 113, 223–243. https://doi.org/10.1016/s0168-1923(02)00109-0.

Xu, G., Xue, X., Wang, P., Yang, Z., Yuan, W., Liu, X., Lou, C., 2018. A lysimeter study for the effects of different canopy sizes on evapotranspiration and crop coefficient of summer maize. Agric. Water Manage. 208, 1–6. https://doi.org/10.1016/j.agwat.2018.04.040.

Yang, P., Hu, H., Tian, F., Zhang, Z., Dai, C., 2016. Crop coefficient for cotton under plastic mulch and drip irrigation based on eddy covariance observation in an arid area of northwestern China. Agric. Water Manage. 171, 21–30. https://doi.org/10.1016/j.agwat.2016.03.007.

Yu, L., Zeng, Y., Su, Z., Cai, H., Zheng, Z., 2016. The effect of different evapotranspiration methods on portraying soil water dynamics and ET partitioning in a semi-arid environment in Northwest China. Hydrol. Earth Syst. Sci. 20, 975–990. https://doi.org/10.5194/hess-20-975-2016.

Yu, L., Zeng, Y., Wen, J., Su, Z., 2018. Liquid-vapor-air flow in the frozen soil. J. Geophys. Res.: Atmos. 123, 7393–7415. https://doi.org/10.1029/2018jd028502.

Zhang, B., Liu, Y., Xu, D., Zhao, N., Lei, B., Rosa, R.D., et al., 2013. The dual crop coefficient approach to estimate and partitioning evapotranspiration of the winter wheat–summer maize crop sequence in North China Plain. Irrig. Sci. 31 (6), 1303–1316. https://doi.org/10.1007/s00271-013-0405-1.

Zhang, Y., Zhao, W., He, J., Zhang, K., 2016. Energy exchange and evapotranspiration over irrigated seed maize agroecosystems in a desert-oasis region, northwest China. Agric. For. Meteorol. 223, 48–59. https://doi.org/10.1016/j.agrformet.2016.04.002.

Zhao, W., Liu, B., Zhang, Z., 2010. Water requirements of maize in the middle Heihe River basin, China. Agric. Water Manage. 97, 215–223. https://doi.org/10.1016/j.agwat.2009.09.011.

Zhao, N., Liu, Y., Cai, J., Paredes, P., Rosa, R.D., Pereira, L.S., 2013. Dual crop coefficient modelling applied to the winter wheat–summer maize crop sequence in North China Plain: basal crop coefficients and soil evaporation component. Agric. Water Manage. 117, 93–105. https://doi.org/10.1016/j.agwat.2012.11.008.

Zhao, H., Shar, A.G., Li, S., Chen, Y., Shi, J., Zhang, X., Tian, X., 2018. Effect of straw return mode on soil aggregation and aggregate carbon content in an annual maize-wheat double cropping system. Soil Tillage Res. 175, 178–186. https://doi.org/10.1016/j.still.2017.09.012.

Zhou, S., Yu, B., Zhang, Y., Huang, Y., Wang, G., 2016. Partitioning evapotranspiration based on the concept of underlying water use efficiency. Water Resour. Res. 52, 1160–1175. https://doi.org/10.1002/2015wr017766.

Zhu, G.-F., Zhang, K., Li, X., Liu, S.-M., Ding, Z.-Y., Ma, J.-Z., Huang, C.-L., Han, T., He, J.-H., 2016. Evaluating the complementary relationship for estimating evapotranspiration using the multi-site data across north China. Agric. For. Meteorol. 230, 33–44. https://doi.org/10.1016/j.agrformet.2016.06.006.